J. Plasma Fusion Res. SERIES, Vol. 6 (2004) 260–262

Two-Dimensional Filamentary Mangnetohydrodynamics, Current-Vortex Method

YATSUYANAGI Yuichi, HATORI Tadatsugu[1], KATO Tomokazu[2] and EBISUZAKI Toshikazu[3]

Kyoto University, Sakyo, Kyoto 606-8501, Japan

[1]Kanagawa University, Hiratsuka, Kanagawa 256-1293, Japan

[2]Waseda University, Shinjuku, Tokyo 169-8555, Japan

[3]RIKEN, Wako, Saitama 351-0198, Japan

(Received: 9 December 2003 / Accepted: 15 June 2004)

Abstract

A two-dimensional filamentary magnetohydrodynamic (MHD) simulation model, current-vortex method, is discussed. In the current-vortex method, a point electric current and a point vortex share the same position on the two-dimensional plane. Time evolution of an MHD system is traced by time evolution of the point electric currents and the point vortices. A viscous effect due to the collisions between the particles may arise in such particle-based simulations. We demonstrate that the (instantaneous) viscosity depends on the number of the particles.

Keywords:

filamentary magnetohydrodynamics, vortex method, current-vortex filament, special-purpose computer, MDGRAPE-2

1. Introduction

We have reported a two-dimensional filamentary magnetohydrodynamic (MHD) simulation model, current-vortex method [1]. The concept is based on the traditional vortex method in hydrodynamics. In the current-vortex method, a point electric current and a point vortex share the same position on the two-dimensional plane. Spatial profiles of the electric current and the vorticity are determined by the sum of such points. Time evolution of an MHD system is traced by time evolution of the magnetic and velocity fields determined by the Biot-Savart integrals of the distributions of the point electric currents and the point vortices. To accelerate the calculations of the Biot-Savart integral, a special-purpose computer for molecular dynamics simulations, MDGRAPE-2, is used [2,3]. The current-vortex method is appropriate for simulations of systems under the high magnetic Reynolds number, because the spatial meshes are not necessary in the current-vortex method. Only the positions of the point electric currents and the point vortices are kept and traced in the simulations.

It should be noted that the particles in the particle-based simulations cause the collisions like ions and electrons. Such collisions yield the viscosity. We demonstrate the viscosity due to the collisions depends on the number of the particles (the point vortices).

In Sec. **2**, we describe the basic equations and the current-vortex method. In Sec. **3**, we explain the numerical viscosity due to the collisions between the point vortices, and demonstrate the numerical results. In Sec. **4**, we give discussions and conclusions.

2. Filamentary magnetohydrodynamics

We use the two-dimensional ideal MHD equations,

$$\frac{\partial \omega_z}{\partial t} = -(\boldsymbol{u}\cdot\nabla)\omega_z + (\boldsymbol{B}\cdot\nabla)j_z, \tag{1}$$

$$\frac{\partial A_z}{\partial t} = -(\boldsymbol{u}\cdot\nabla)A_z, \tag{2}$$

$$\nabla\cdot\boldsymbol{u} = 0, \tag{3}$$

$$\boldsymbol{E} + \boldsymbol{u}\times\boldsymbol{B} = 0, \tag{4}$$

$$\boldsymbol{B} = -\hat{z}\times\nabla A_z, \tag{5}$$

$$\omega_z = \hat{z}\cdot\nabla\times\boldsymbol{u}, \tag{6}$$

$$j_z = \frac{\hat{z}}{\mu_0}\cdot\nabla\times\boldsymbol{B}, \tag{7}$$

where $\boldsymbol{B}$ and $\boldsymbol{u}$ are the magnetic field and the velocity on the x-y plane, A_z, j_z and ω_z are the z components of the magnetic vector potential, the electric current density and the vorticity, respectively. The unit vector in z direction is denoted by $\hat{z}$. The mass density is normalized to unity.

We assume that the electric current $j_z(\boldsymbol{r},t)$ and the vorticity $\omega_z(\boldsymbol{r},t)$ have discontinuous distributions,

Corresponding author's e-mail: yyanagi@phys.h.kyoto-u.ac.jp

$$j_z(\boldsymbol{r},t)=\sum_i J_i(t)\delta(\boldsymbol{r}-\boldsymbol{r}_i(t)), \tag{8}$$

$$\omega_z(\boldsymbol{r},t)=\sum_i \Omega_i(t)\delta(\boldsymbol{r}-\boldsymbol{r}_i(t)), \tag{9}$$

where $\delta(\boldsymbol{r})$ is the two-dimensional Dirac delta function. Notations $J_i(t)$, $\Omega_i(t)$ are the total electric current and the circulation inside the i-th current-vortex filament pointed by the position vector $\boldsymbol{r}_i(t)$, respectively. They are confined in each filament coaxially. Following the above expressions, magnetic field $\boldsymbol{B}(\boldsymbol{r},t)$ and velocity field $\boldsymbol{u}(\boldsymbol{r},t)$ are defined as follows:

$$\boldsymbol{B}(\boldsymbol{r},t)=\sum_i J_i(t)\nabla G(\boldsymbol{r}-\boldsymbol{r}_i(t))\times\hat{z}, \tag{10}$$

$$\boldsymbol{u}(\boldsymbol{r},t)=\sum_i \Omega_i(t)\nabla G(\boldsymbol{r}-\boldsymbol{r}_i(t))\times\hat{z}. \tag{11}$$

The function G($\boldsymbol{r}$) is the two-dimensional Green function for the Poisson equation. The right hand sides of eqs. (10) and (11) are the Biot-Savart integrals in the discretized form.

We rewrite the vorticity equation (1) and the magnetic induction equation (2) in terms of the filamentary representations (8)–(11). Details are given in ref. [1]. The obtained equations are

$$\frac{\mathrm{d}\boldsymbol{r}_k}{\mathrm{d}t}=\boldsymbol{u}(\boldsymbol{r}_k,t)-\frac{J_k(t)}{\Omega_k(t)}\boldsymbol{B}(\boldsymbol{r}_k,t), \tag{12}$$

$$\frac{\mathrm{d}\Omega_k(t)}{\mathrm{d}t}=0, \tag{13}$$

$$\frac{\mathrm{d}J_k(t)}{\mathrm{d}t}=0. \tag{14}$$

Equations (12), (13) and (14) are the equation of motion, the conservation of circulation and the conservation of total electric current of the k-th filament, respectively.

3. Viscous effect

In this section, we discuss the viscous effect in particle simulations. Here we limit ourselves to the pure hydrodynamic case, i.e., $J_k(t) = 0$ in eq. (12) for simplicity. In this limit, the current-vortex method exactly coincides with the traditional point vortex method.

The point vortex method gives the analytically correct solution to two-dimensional incompressible Euler equation [4]. On the other hand, in the limit of infinite number of point vortices, the discontinuous vorticity field (9) converges to the continuous one. In this limit, the equations of the point vortex method converge to the Euler equation for continuous fluids [5]. However, it appears that using an increased number of vortices of decreased strength will not yield a converged solution in numerical simulations [6]. This may be due to the viscosity that originates with the collisions between the point vortices, even if there is no explicit viscous diffusion term in the Euler equation. Such viscosity does not arise in the mesh-based simulations for the continuous fluids, because there is no collisional process in the macroscopic fluid scale in the Euler equation.

In the model, we neglect the viscous parameters, i.e., the electric resistivity and the kinetic viscosity. Thus, all the viscous effects in the simulations come from the numerical ones. The following relation is used to determine the (instantaneous) numerical viscosity from the total kinetic energy H and the enstrophy Γ,

$$\frac{\mathrm{d}H}{\mathrm{d}t}=-\eta\Gamma, \tag{15}$$

where

$$H=\frac{1}{2}\int \boldsymbol{u}^2(\boldsymbol{r},t)\mathrm{d}\boldsymbol{r}, \tag{16}$$

$$\Gamma=\frac{1}{2}\int \omega_z^2(\boldsymbol{r},t)\mathrm{d}\boldsymbol{r}, \tag{17}$$

To check the numerical viscous effect, the simulation results of the diocotron instability in the magnetized pure electron plasmas are used [7]. It is analytically shown that the two-dimensional equations of motion of low-density non-neutral electron plasmas with the guiding-center approximation coincide with those of the two-dimensional nonmagnetized fluids, i.e., the Euler equation. Thus, the time evolution of the pure electron plasmas can be traced by the point vortex method. In this system, velocity $\boldsymbol{u}$ in energy H is determined by eq. (11). Enstrophy Γ is determined by

$$\Gamma=\int\left(\nabla^2\psi(\boldsymbol{r},t)^2\right)\mathrm{d}\boldsymbol{r}, \tag{18}$$

$$\psi(\boldsymbol{r},t)=\sum_i \Omega_i(t)\mathrm{G}(\boldsymbol{r}-\boldsymbol{r}_i(t)), \tag{19}$$

where $\psi(\boldsymbol{r},t)$ is stream function for the two-dimensional flow. Note that the enstrophy is not well defined in the point vortex system. Thus the enstrophy is determined by the stream function $\psi(\boldsymbol{r},t)$ that is well defined even in the point vortex system. To evaluate the viscosity η numerically, we use eq. (15) in the following form,

$$\eta=\frac{H(t)-H(0)}{t\Gamma(t)}, \tag{20}$$

becasue there are very small fluctuations in $H(t)$ obtained by the simulation results and it is difficult to evaluate the instantaneous value of $\mathrm{d}H(t)/\mathrm{d}t$ exactly.

Initial conditions are as follows. Initial ratio of the inner to the outer radii of the annular electron distribution is 0.6. There is no conducting wall around the electrons. We compare the simulation results where total numbers of the point vortices are 1.0×10^4, 4.0×10^4, 6.0×10^4 and 8.0×10^4. In these simulations, the values of the circulation are equal. Time evolutions of the instantaneous viscosity are plotted in Fig. 1.

In Fig. 1, linear growth stage is $T = 30 - 90$. In this period, annular electron layer develops into clumps. After the linear growth stage, the clumps are merged and the electron distribution shows broad one. Then, the electrons are transferred by the near-steady circular flow and there may be less collisional processes than the initial stage. Thus the phenomenon in the linear growth stage is more important than that in the nonlinear stage for us to reveal the mechanism of the viscosity due to the collisions.

In the linear growth stage, the viscosity in the 1.0×10^4

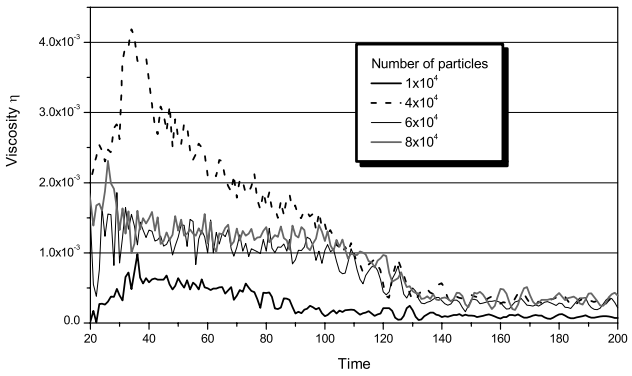

Fig. 1 Time evolutions of the instantaneous viscosity are plotted.

particles case is minimum, and the maximum viscosity corresponds to the 2.0×10^4 particles case. In addition, during all the simulation time, the 1.0×10^4 particles case shows the lowest viscosity. Thus we conclude that the viscosity is due to the collisional process of the point vortices, even if there is no explicit viscous diffusion term in the Euler equation. On the other hand, the viscosity due to the collisions should converge to zero for the continuous fluid, i.e., in the limit of infinite number of vortices. In the 6.0×10^4 and 8.0×10^4 particles cases, the values of the viscosity is larger than the 1.0×10^4 particles case, but smaller than the 2.0×10^4 particles case. Thus it is likely that the viscosity increases as the number of vortices n increases upto a cirtain critical value, say n_0, and decreases for larger $n (> n_0)$. The value of n may be between 1.0×10^4 and 6.0×10^4. Note that the viscosity does not yet converge to zero in the simulation results. It is very difficult to demonstrate the zero-viscosity result by the simulation.

4. Discussion and conclusion

We have presented the simulation model where the electric current and the vorticity are discretized in the same manner as the traditional vortex method in hydrodynamics. Time evolution of an MHD system is traced by time evolution of the magnetic and velocity fields determined by the Biot-Savart integrals of the distributions of the point electric currents and the point vortices. To accelerate the calculations of the integral, MDGRAPE-2 has been used. The model is suitable for the simulations of the high magnetic Reynolds number.

We have demonstrated that the viscosity depends on the number of vortices. It seems likely that the value approaches to zero at infinite number of point vortices, though it is not yet demonstrated by the simulations. It is nessesary to determine the critical value of the number of vortices where the viscosity due to the collisional effect becomes maximum. We are now analytically evaluating the viscosity on the current-vortex method.

References

[1] Y. Yatsuyanagi *et al.*, Phys. Plasmas **10**, 3181 (2003).
[2] T. Narumi *et al.*, Mol. Simul. **21**, 401 (1999).
[3] R. Susukita *et al.*, Comput. Phys. Comm. **155**, 115 (2003).
[4] J.P. Christiansen, J. Comput. Phys. **135**, 189 (1997).
[5] J. Goodman, T.Y. Hou and J. Lowengrub, Comm. Pure Appl. Math. **43**, 415 (1990).
[6] A. Leonard, J. Comput. Phys. **37**, 289 (1980).
[7] Y. Yatsuyanagi *et al.*, Phys. Plasmas **10**, 3188 (2003).